Structural and luminescence properties of Ge nanocrystals before and after an ion irradiation process

¹F. Nornberg, ²F. L. Bregolin, ^{1,2}U. S. Sias francielefnornberg@gmail.com, uilson@pelotas.ifsul.edu.br

¹ Instituto Federal de Educação, Ciência e Tecnologia Sul-rio-grandense – Campus Pelotas, 96015-370, Pelotas, RS, Brazil ² Instituto do Física, Universidado Federal do Rio Grando do Sul C.P. 15051, 91501.

² Instituto de Física, Universidade Federal do Rio Grande do Sul C.P. 15051, 91501-970, Porto Alegre, RS, Brazil

Abstract

In this work, SiO₂ layers containing Ge nanocrystals (NCs) obtained by the hot implantation approach were submitted to an ion irradiation process with different 2 MeV Si⁺ ion fluences. We have investigated the Photoluminescence (PL) behavior and structural properties of the irradiated samples as well as the features of the PL and structural recovery after an additional thermal treatment. We have shown that even with the highest ion bombardment fluence employed (2x10¹⁵ Si/cm²) there is a residual PL emission (12 % from the original) and survival of some Ge NCs is still observed by Transmission electron microscopy analysis. Even though the final PL and mean diameter of the nanoparticles under ion irradiation are independent of the implantation temperature or annealing time, the PL and structural recovery of the ion-bombarded samples have a memory effect. We have also observed that the lower the ion bombardment fluence, the less efficient is the PL recovery. We have explained such behavior based on current literature data.

1. Introduction

First experiments using ion implantation as a technique to produce Si or Ge nanocrystals (NCs) in order to study their electro-optical properties were already reported in the early 90's [1-3] and the promising results, motivated by the possible applications in electronic and photonic devices, were followed by an intense research activity, as illustrated by the review of Rebohle et al. [4]. Commonly, photoluminescence (PL) from Ge nanocrystals (NCs) has been obtained by room temperature (RT) Ge implantation into a SiO₂ matrix followed by a high temperature anneal [4,5].

Few years ago, we have reported interesting results about the optical and structural properties of Si NCs embedded into SiO_2 matrix, obtained with the substrate kept at high temperature (hot implantation) during the Si implantation process [6,7]. Recently, motivated by the results observed with Si NCs in SiO_2 , we have studied the PL behavior from Ge NCs produced using the hot implantation approach and preliminary results were published in a conference proceeding paper [8]. However, at that moment, we did not have an explanation for the enhancement in the PL yield and we have proposed that transmission electron microscopy (TEM) analysis could elucidate the above-described feature.

We have undertaken the present work with two main goals: First, to perform a structural characterization of the samples, comparing the Ge NCs distributions obtained by implantation at RT and further anneal at 900 °C with those obtained by hot implantation, after the 900 °C anneal. Based on these experiments, we intend to explain the PL enhancement observed in the hot implanted samples. Second, to study the PL behavior of the samples under an ion irradiation process as well as the subsequent further annealing used to recover the PL emission. These measurements are also followed by TEM analysis, in order to observe the structural changes that occur during the PL quenching and recovery process.

2. Experimental procedure

A 320 nm-thick SiO_2 layer, thermally grown onto a Si < 100 > wafer, was implanted with 120 keV Ge ions keeping constant the substrate temperature from RT up to 600 °C. The implantation was done at a fluence of 1.2×10^{16} Ge/cm², corresponding to a Gaussian-like depth profile with a peak concentration of about 3 at %. The as-implanted samples were then annealed at 900 °C for 1 h in order to grow the Ge NCs. The thermal annealing was performed in different atmospheres (N_2 , Ar and forming gas) using a quartz-tube furnace with times varying from 1 h to 3 h. Afterwards, we have bombarded the Ge NCs with a 2 MeV Si^+ beam with fluences ranging from 2×10^{11} to 2×10^{15} Si/cm² searching for the PL quenching. Subsequently, we have annealed the samples at 900 °C additionally for 1 h, in order to recover the PL yield. The PL measurements were performed at RT, using a Xe lamp monochromated at 240 nm (5.1 eV) as an excitation source. The

sample emission was dispersed by a 0.3 m single spectrometer and detected with a CCD. The structural characterization was performed by transmission electron microscopy (TEM) using a 200 keV JEOL microscope with the samples prepared in a cross sectional mode by mechanical polishing and ion milling techniques.

3. Results

3.1. Hot implantation effect: PL emission and TEM results

In Fig. 1, are shown the PL spectra of samples implanted at RT and 350 °C with a fluence of 1.2x10¹⁶ Ge/cm² and further annealed at 900 °C by 1 h. The inset illustrates the evolution of the emission yield as a function of the substrate temperatures used in the implantation process. Although all hot implanted samples present a PL yield higher than the RT implanted ones, the PL shape is similar. From now, we will report on the results of samples implanted at RT and 350 °C, which presents the highest PL yield.

The TEM measurements reveal the formation of crystalline Ge nanoclusters in both RT and hot implanted samples after the 900 °C anneal, as shown in Fig. 2a) and b), respectively. For the RT implanted sample (Fig. 2a) we have found a Gaussian–like NCs size distribution with large clusters located at the center of the implantation profile and smaller ones towards the edges of the distribution. Concerning the hot implanted samples (Fig. 2b), the mean size and size distribution differ significantly. In fact, the Ge NCs distribution presents a positive gradient profile of particle sizes along depth. However, when we calculate the mean diameter of both size distributions we obtained a larger value for the RT implanted sample, 3.6 nm, against 3.0 nm for the hot implanted one, as displayed by the corresponding histograms in Fig. 2 c) and d), respectively.

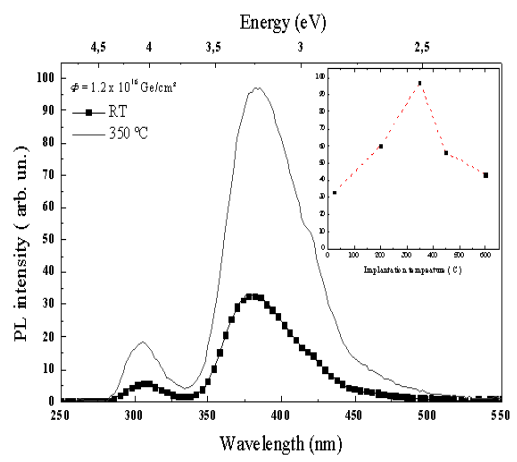


Fig. 1. PL spectra from samples implanted at RT (symbols) and 350 °C (line) with a fluence Φ =1.2x10¹⁶ Ge/cm² annealed at 900 °C by 1 h. The inset shows maximum PL yield as a function of the implantation temperature.

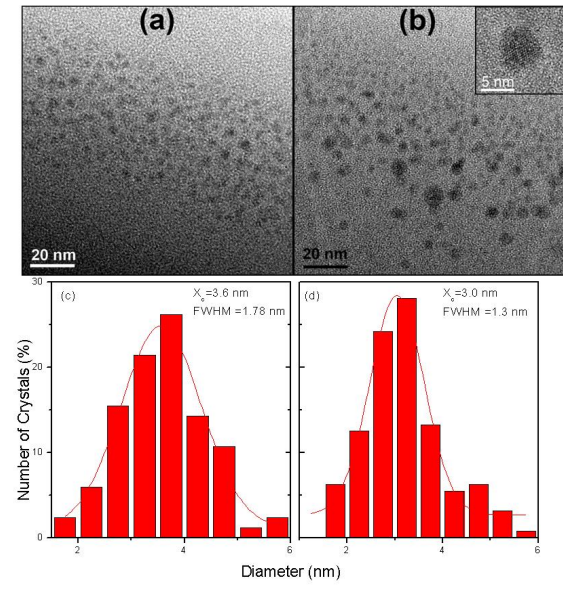


Fig. 2. Detailed TEM view showing the NCs size distribution for a) RT implantation b) high temperature implantation (samples implanted to $\Phi = 1.2 \times 10^{16} \text{ Ge/cm}^2$ and annealed at 900 °C by 1 h). Corresponding histograms: c) RT implanted sample and d) hot implanted sample.

3.2. Irradiation and post-annealing results

In this experiment, samples implanted with a fluence of $\Phi = 1.2 \times 10^{16}~\text{Ge/cm}^2$ and annealed for 1 h (pristine sample) were submitted to an ion bombardment process with a 2 MeV Si⁺ beam with fluences between $2 \times 10^{12}~\text{Si/cm}^2$ and $2 \times 10^{15}~\text{Si/cm}^2$. The chosen energy is high enough to irradiate the whole SiO₂ film.

In Fig. 3a, we show the evolution of the PL spectrum of hot implanted samples (Ti=350 °C) submitted to different ion irradiation fluences. In comparison to the non-irradiated sample (pristine sample), it can be observed that the PL yield diminishes with increasing irradiation fluences. For fluences higher than $2x10^{14}$ Si/cm² the PL spectrum reaches a minimum yield (12 % from the original) with the same line shape and intensity, as the spectrum of the sample irradiated with $2x10^{15}$ Si/cm². In sequence, in Fig. 3b is shown the PL recovery behavior of the corresponding samples under an additional 1 h anneal at 900 °C. The pristine sample was also submitted to the additional thermal treatment resulting in a sample annealed by 2 h. As can be

observed in Fig. 3b, the higher the irradiation fluence applied to the pristine sample, the more efficient the PL recovery.

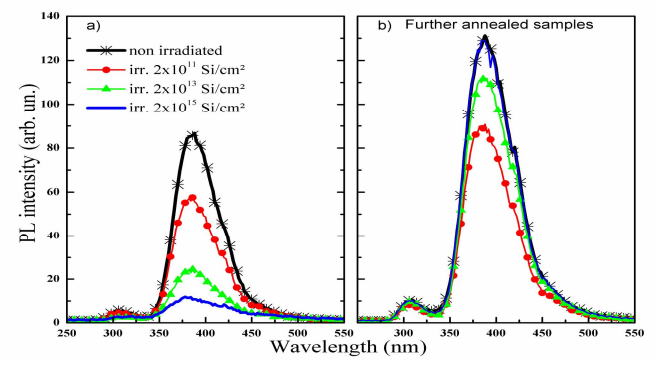


Fig. 3. a) PL spectra of samples after an irradiation process with Si ions at different fluences. b) PL spectra of the irradiated samples after a further annealing at 900 °C by 1 h. Black Line and symbols represent the PL spectrum of the sample implanted at 350 °C with a fluence of 1.2×10^{16} Ge/cm² and annealed at 900 °C without irradiation.

3.3. TEM analysis

It is important to point out that even for samples bombarded with the highest fluence we have still observed surviving nanocrystals, as evidenced by the high-resolution TEM (HRTEM) micrograph in Fig. 4.

In Fig. 5, we show (on the left) the histograms from TEM observations of a hot implanted and RT pristine samples that were irradiated with a fluence of $2x10^{15}$ Si/cm² (Fig. 5 (a) and (b)). On the bottom of the Fig. 5 are shown the corresponding histograms of the irradiated samples after proceeding an additional anneal at 900 °C by 1 h (Fig 5 (c) and (d)).

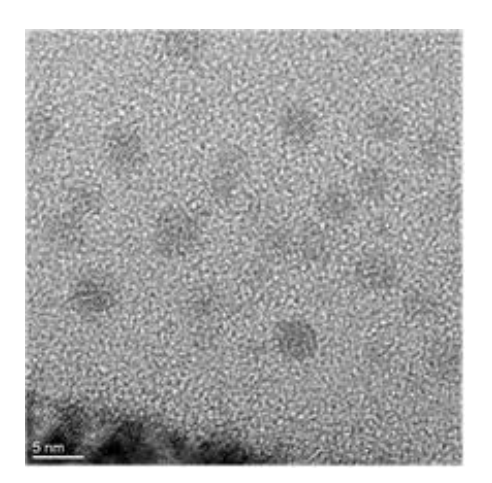


Fig. 4. HRTEM image showing Ge NCs embedded in a SiO_2 matrix. It corresponds to a sample implanted at 350 °C with a fluence of 1.2×10^{16} Ge/cm² and annealed by 1 h that was irradiated with a 2 MeV Si⁺ ions at a fluence of 2×10^{15} Si/cm².

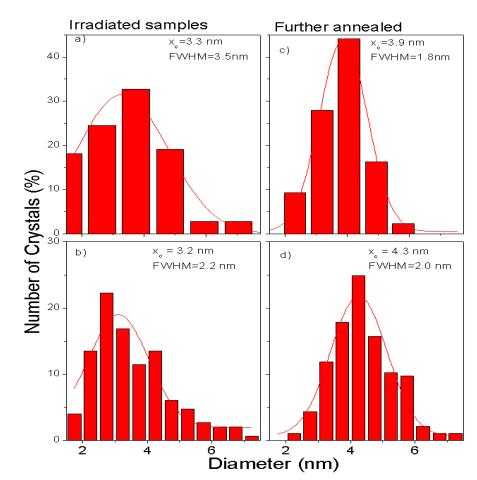


Fig. 5. (On the left) Size histograms from TEM micrographs of: (a) hot implanted and (b) RT pristine samples irradiated with 2x10¹⁵ Si/cm². (On the right) Corresponding size histograms of further annealed samples after the irradiation process: (c) hot and (d) RT implanted samples.

By comparing the results presented in Fig. 5, we can verify that the mean diameter of both samples converge to the same value after the irradiation process (~3.2 nm). On the other hand, the further anneal of the corresponding samples (on the right side of Fig. 5) shows as a result, histograms with a more uniform size, presenting the same mean diameter values (3.9 nm and 4.3 nm for the hot and RT implanted samples, respectively) as compared to the pristine samples (without irradiation), but with 2 h of annealing. It is reasonable, because the irradiated samples had an additional hour at 900 °C in order to recover the PL yield. We would like to mention that when we submitted a pristine sample (RT or hot implanted) annealed by 2 h to the irradiation process, the resulting mean diameter was also ~3.2 nm, since the amount of Ge in the SiO₂ matrix is independent of the implantation temperature. Table 1 shows a summary of the present results for the mean diameters obtained from the histograms of the TEM observations. An important feature to point out is that the evolution of the system with the annealing time after the irradiation process continues depending on

the temperature that the samples were implanted, because the final mean diameter is equivalent to the corresponding pristine samples (RT and hot implanted ones) with 2 h of annealing –see table 1.

Tab. 1. Size histograms from TEM analysis

Description	Mean diameter (nm) (± 5%)	
	Hot-implanted	RT
1 h-annealed	3.0	3.6
1 h-annealed and further	3.3	3.2
irradiated and 1 h further	3.9	4.3
2 h-annealed	3.9	4.3
2 h-annealed and further	3.3	3.3

4. Discussion and conclusions

The nature of the PL bands in this system is well known, being attributed to radiative defects present at the Ge NCs/matrix interface, specifically, neutral oxygen vacancies (NOV) like \equiv Ge-Si \equiv and/or \equiv Ge-Ge \equiv defects generated by the local deficiency of oxygen and the incorporation of Ge into the SiO₂ network surrounding the NCs [2, 4, 5, 9].

The hot implantation approach has given an increase of a factor of three in the PL yield, as compared with the one obtained by RT implantation. By TEM analysis, we have shown that the Ge NCs produced by hot implantation have a mean diameter size (3.0 nm) smaller than the corresponding ones produced by RT implantation (3.6 nm). Since the surface to volume ratio is larger for smaller precipitates, then, more Ge atoms contribute to form NOV defects centers at the NC/matrix interface, consequently giving place to a higher PL yield, as illustrated in Fig. 1.

In Ge NCs in SiO_2 , although we have observed survival nanocrystals even after the highest irradiation fluence of $2x10^{15}$ Si/cm^2 –see Fig. 4, the residual PL emission (Fig. 3a) is probably associated to the remaining radiative centers related to Ge–Ge and/or Si–Ge bonds, which survived the irradiation process. Further, the large number of non-radiative defects generated in the matrix during the ion bombardment also contributes significantly to the reduction of the PL yield.

Concerning the TEM analysis after the irradiation process, we have observed that the resultant mean diameter after ion irradiation is practically the same independent of the implantation temperature of the sample. This feature can be clarified based on the fact that the Ge excess is the same in both samples, also independent of the annealing time. Then, when the system is perturbed with this high fluence of Si ions, the size distribution converges to a similar configuration at the end of the irradiation process. However, the memory of the size distribution is conserved, since the mean diameter and size distribution have the same characteristics of the pristine samples (RT and hot implanted) annealed for an additional hour – see Table 1. This can be attributed to the fact that the irradiation process mostly acts in the fragmentation of the nanoparticles and does not contribute to a redistribution of the Ge content due to irradiation-induced diffusion. The PL recovery is in agreement with the above statement, since for the irradiated samples the PL yield increases after the post-annealing, reaching the same value of the pristine sample annealed additionally by one hour.

In Fig. 3b is observed that the lower the irradiation fluence, the less efficient is the PL recovery. We can explain this feature by a selective effect of the ion bombardment on the nanoparticles. The global effect at low ion irradiation fluences is more pronounced on the smaller nanoparticles, which are the main source of the PL emission and have a surface/volume ratio higher than the larger ones. This statement has a support in a work that uses a combination of molecular dynamics (MD) simulations and x-ray absorption spectroscopy (XAS) to study the amorphization of Ge and Si NCs embedded in amorphous SiO₂ by ion irradiation, published by M. Backman et al. [10]. There they show that, the susceptibility to amorphization decreases with increasing nanocrystal size. In our case, after the post-annealing, the fragments of these smaller nanoparticles could agglutinate, resulting in an increase in the mean size of the overall distribution, which would diminish the PL efficiency.

On the other hand, for larger nanoparticles a higher number of incident ions is necessary to provide a considerable fragmentation of them, which, after the further annealing, would turn enable the formation of smaller nanoparticles as an overall result and a consequent increase in the PL efficiency.

A last issue to point out is that we have observed by TEM analysis the survival of some Ge NCs even under the highest ion irradiation fluence of $2x10^{15}$ Si/cm² –see Fig. 4. This observation is at variance with the results published by Djurabekova et al. in a study about the behavior of bulk and nanostructured Ge under ion irradiation with 5 MeV Si⁺ ions, at liquid nitrogen temperature [11]. By Extended X-ray Absorption Fine Structure (EXAFS) experiments, they have observed a clear amorphization of Ge NCs already with the fluence

of $2x10^{13}$ Si/cm². This divergence could be attributed to the different irradiation energies and substrate temperatures used during the irradiation process in each experiment.

5. References

- [1] T. Shimizu-Iwayama, K. Fujita, S. Nakao, K. Saitoh, T. Fujita, and N. Itoh, J. Appl. Phys. 75, 7779 (1994).
- [2] L. Rebohle, J. von Borany, R. A. Yankov, W. Skorupa, I. E. Tyschenco, H. Fröb and K. Leo, Appl. Phys. Lett. 71, 2809 (1997).
- [3] K. V. Shcheglov, C. M. Yang, K. J. Vahala, and Harry A. Atwater, Appl. Phys. Lett. 66, 745 (1995).
- [4] L. Rebohle, J. von Borany, H. Fröb and W. Skorupa, App. Phys. B: Laser and Optics. 71, 131 (2000).
- [5] J. M. J. Lopez, F. C. Zawislak, M. Behar, P. F. P. Fichtner, L. Rebohle, W. Skorupa, J. Appl. Phys. 94, 6059, (2003) and references there in.
- [6] U. S. Sias, E. C. Moreira, E. Ribeiro, H. Boudinov, L. Amaral and M. Behar, J. App. Phys. 95, 5053 (2004).
- [7] U. S. Sias, L. Amaral, M. Behar, H. Boudinov, E. C. Moreira and E. Ribeiro, J. App. Phys. 98, 0341312 (2005).
- [8] F.L. Bregolin, M. Behar, U.S. Sias and E.C. Moreira, Nucl. Instrum. and Meth. B, 267, 1321 (2009).
- [9] Y.H. Ye, J.Y. Zhang, X.M. Bao, X.L. Tan, L.F. Chen: Appl. Phys. A 67, 213 (1998).
- [10] M. Backman, F. Djurabekova, O. H. Pakarinen, K. Nordlund, L. L. Araujo, and M. C. Ridgway, Phys Rev. B, 80, 144109 (2009).
- [11] F. Djurabekova, M. Backman, O. H. Pakarinen, K. Nordlund, L. L. Araujo and M.C. Ridgway, Nucl. Instrum. and Meth. B, 267, 1235 (2009).